0026-895X/03/6303-538–546$7.00
MOLECULAR PHARMACOLOGY
Vol. 63, No. 3
2167/1047489
Mol Pharmacol 63:538–546, 2003
Printed in U.S.A.

Structural Analysis of the Activation of Ribavirin Analogs by NDP Kinase: Comparison with Other Ribavirin Targets

SARAH GALLOIS-MONTBRUN, YUXING CHEN, HÉLÈNE DUTARTRE, MAGALI SOPHYS, SOLANGE MORERA, CATHERINE GUERREIRO, BENOIT SCHNEIDER,[1] LAURENCE MULARD, JOËL JANIN, MICHEL VERON, DOMINIQUE DEVILLE-BONNE, and BRUNO CANARD

Unité de Régulation Enzymatique des Activités Cellulaires, Centre National de la Recherche Scientifique (CNRS) Formation de Recherche en Evolution 2364, Institut Pasteur, Paris, France (S.G.-M., B.S., M.V., D.D.-B.); Laboratoire d'Enzymologie et de Biochimie Structurales, CNRS Unité Propre de Recherche 9063, Gif-sur-Yvette, France (Y.C., S.M., J.J.); Laboratoire d'Architecture et Fonction des Macromolecules Biologiques, CNRS Unité Mixte de Recherche 6098, Ecole Supérieure d'Ingénieurs de Luminy, case 925, Marseille, France (H.D., M.S., B.C.); and Unité de Chimie Organique, CNRS Unité de Recherche Associée 2128, Institut Pasteur, Paris, France (C.G., L.M.)

Received September 23, 2002; accepted December 6, 2002

This article is available online at http://molpharm.aspetjournals.org

ABSTRACT

Ribavirin used in therapies against hepatitis C virus (HCV) is potentially efficient against other viruses but presents a high cytotoxicity. Several ribavirin triphosphate analogs modified on the ribose moiety were synthesized and tested in vitro on the RNA polymerases of HCV, phage T7, and HIV-1 reverse transcriptase. Modified nucleotides with 2′-deoxy, 3′-deoxy, 2′,3′-dideoxy, 2′,3′-dideoxy-2′,3′-dehydro, and 2′,3′-epoxy-ribose inhibited the HCV enzyme but not the other two polymerases. They were also analyzed as substrates for nucleoside diphosphate (NDP) kinase, the enzyme responsible for the last step of the cellular activation of antiviral nucleoside analogs. An X-ray structure of NDP kinase complexed with ribavirin triphosphate was determined. It demonstrates that the analog binds as a normal substrate despite the modified base and confirms the crucial role of the 3′-hydroxyl group in the phosphorylation reaction. The 3′-hydroxyl is required for inhibition of the initiation step of RNA synthesis by HCV polymerase, and both sugar hydroxyls must be present to inhibit elongation. The 2′deoxyribavirin is the only derivative efficient in vitro against HCV polymerase and properly activated by NDP kinase.

Ribavirin is a broad-spectrum antiviral agent discovered in 1972 (Witkowski et al., 1972). It is used in therapy against chronic hepatitis C virus (HCV) infection in combination with interferon α (McHutchison et al., 1998; Poynard et al., 1998). It is also of potential interest against poliovirus, Lassa fever virus, respiratory syncytial virus, and emerging viruses, such as West Nile virus, but the exact mode of action of ribavirin remains uncertain (Patterson and Fernandez-Larsson, 1990). It may be indirect, through the inhibition of cellular IMP dehydrogenase, resulting in a decrease of the guanine nucleotide pool. Alternatively, ribavirin may directly target the replication of RNA viruses, acting as an analog of purine nucleosides. Ribavirin 5′-triphosphate (RTP) is an inhibitor of the replicative RNA polymerases of influenza virus (Wray et al., 1985), poliovirus (Crotty et al., 2000), and vesicular stomatitis virus (Patterson and Fernandez-Larsson, 1990). It is a substrate for the polymerases of poliovirus (Crotty et al., 2000) and HCV (Maag et al., 2001). These enzymes incorporate ribavirin in the viral RNA facing either cytosine or uracil. Although the efficiency of incorporation is decreased by a factor in the 10^4 to 10^5 range compared with natural purine nucleotides, the analog is a powerful mutagen and the accumulation of replicative errors may explain its antiviral effect (Crotty et al., 2000).

Ribavirin transport into cells is probably mediated by nucleoside transporters (Jarvis et al., 1998; Patil et al., 1998). Intracellular phosphorylation is required for antiviral activity and must reach the 5′-triphosphate level for incorporation by RNA polymerases. Phosphorylated anabolites (ribavirin mono-, di-, and triphosphates) are observed in erythrocytes because of the action of adenosine kinase (Page and Conner, 1990; Homma et al., 1999) and other kinases of the salvage nucleotide pathway. These include nucleoside diphosphate

This work was supported by Ministere de l'Education Nationale, Ministere de la Recherche et de la Technologie (Program Microbiologie, Maladies Infectieuses et Parasitaires), by Association pour la Recherche contre le Cancer, and by Association Nationale de Recherche contre le Sida (ANRS) and by Sidaction-Ensemble contre le SIDA.

S.G.-M., Y.C., and H.D. contributed equally to this work.

[1] Current address: Laboratoire de Differenciation Cellulaire et Prions, CNRS-UPR 1983, 7 Rue Guy Môquet, 94801 Villejuif Cedex, France.

ABBREVIATIONS: HCV, hepatitis C virus; NDP, nucleoside diphosphate; d4T, 2′,3′-dideoxy-2′,3′dehydrothymidine; RMP, ribavirin monophosphate; ddR, 2′,3′-dideoxyribavirin; d4R, 2′,3′-didehydro-2′,3′-dideoxyribavirin; epoxyR, 2′,3′-anhydroribavirin; 2′dR, 2′-deoxyribavirin; HPLC, high-performance liquid chromatography; DTT, dithiothreitol; PEG, polyethylene glycol; RTP, ribavirin triphosphate; HIV, human immunodeficiency virus; RT, reverse transcriptase; RNAP, RNA polymerase; RMS, root-mean-square; ddRTP, 2′,3′-dideoxyribavirin triphosphate; epoxyRTP, 2′,3′-anhydroribavirin triphosphate.

(NDP) kinase, which produces the triphosphate form by transferring the γ-phosphate of a nucleoside triphosphate (usually ATP) via a covalent phosphohistidine intermediate (Parks and Agarwal, 1973). NDP kinase has a high catalytic efficiency and a broad specificity, taking as substrates all natural diphosphate nucleosides and deoxynucleosides. It also phosphorylates the diphosphate derivatives of several antiviral nucleoside analogs such as 3′-azidothymidine and 2′,3′-dideoxy-2′,3′-didehydrothymidine (d4T), but with a much lower efficiency (Bourdais et al., 1996). These analogs, which are chain terminators in DNA synthesis, lack a 3′-OH group. Because the latter has been shown to play a major role in catalysis by NDP kinase (Schneider et al., 1998), ribavirin, which contains an unmodified ribose, should be more efficiently activated.

A major problem with ribavirin in therapy is its high cellular toxicity. This is possibly related to the inhibition by ribavirin monophosphate (RMP) of IMP dehydrogenase, which catalyzes the oxidation of IMP into xanthosine monophosphate, the rate-limiting step of the de novo synthesis of guanine nucleotides. The structural and functional properties of IMP dehydrogenase have been studied extensively (Sintchak and Nimmesgern, 2000), and X-ray structures are available (Colby et al., 1999). RMP probably mimics IMP. With the aim of decreasing its toxicity and improving the antiviral properties of ribavirin, we investigate here the action of NDP kinase on phosphorylated ribavirin derivatives. The enzymatic analysis is supported by an X-ray structure of NDP kinase in complex with ribavirin triphosphate. We also prepared ribavirin analogs bearing modifications on the 2′-OH and/or the 3′-OH of the ribose moiety, study their properties as NDP kinase substrates and their ability to inhibit viral polymerases, HIV-1 reverse transcriptase and T7 RNA polymerase, as well as the HCV polymerase, the RNA polymerase of the hepatitis C virus.

Materials and Methods

Synthesis of Ribavirin Triphosphate Analogs. Analytically pure ribavirin was either a kind gift from Pr. Chris Meier (Hamburg, Germany) or was purchased from ICN Pharmaceuticals. 2′,3′-Dideoxy-2′,3′-didehydroribavirin (d4R), 2′,3′-dideoxyribavirin (ddR), and 2′,3′-anhydro-ribavirin (epoxyR) (Fig. 1) were synthesized from ribavirin according to the procedures described by Upadhya et al. (1990). 2′-Deoxyribavirin (2′dR) (Pochet and Dugué, 1998) and 3′-deoxyribavirin (3′dR) (Upadhya et al., 1990) were obtained in four steps by radical deoxygenation of appropriately bis-silylated ribavirin at position 2′ and 3′, respectively, as described for the preparation of the 3′-deoxyadenosine (Meier and Huynh-Dinh, 1991). Conversion of ribavirin and analogs into their corresponding triphosphate was performed according to the method of Ludwig and Eckstein (1989). Spectra from electrospray ionization mass spectrometry were recorded in the negative-ion mode. HPLC analyses were performed on a PerkinElmer series 200 unit using a reverse-phase analytical column (Uptisphere UPS HDO, C18, 120 Å, 4.6 × 250 mm, 5 μm; Interchim, Montluçon, France) with detection at 230 nm. The eluants used were acetonitrile/10 mM triethylammonium acetate buffer, pH 6.6, 1/19 (A) and acetonitrile/10 mM triethylammonium acetate buffer, pH 6.6, 3/17 (B). A linear gradient from A to B over 20 min was used with a flow rate of 1 ml/min. Characteristic data for the target compounds are as follows: ribavirin 5′-triphosphate: HPLC, 4.91 min; $C_8H_{15}N_4O_{14}P_3$ (483.98) m/z 483 (M-H); 2′-deoxyribavirin 5′-triphosphate: HPLC, 5.56 min; $C_8H_{15}N_4O_{13}P_3$ (467.98) m/z 467 (M-H); 3′-deoxyribavirin 5′-triphosphate: HPLC, 4.87 min; $C_8H_{15}N_4O_{13}P_3$ (467.98) m/z 467 (M-H); 2′,3′-dideoxy-2′,3′-didehydroribavirin 5′-triphosphate: HPLC, 5.99 min; $C_8H_{11}N_4O_{12}P_3$ (449.97) m/z 449 (M-H); 2′,3′-dideoxyribavirin 5′-triphosphate: HPLC, 6.01 min, $C_8H_{15}N_4O_{12}P_3$ (451.99) m/z 451 (M-H); and 2′,3′-anhydroribavirin 5′-triphosphate: HPLC, 5.79 min; $C_8H_{13}N_4O_{13}P_3$ (465.97) m/z 465 (M-H).

Expression and Purification of NDP Kinases. Human NDP kinase A was purified as a recombinant protein overexpressed in *Esherichia coli* (BL21-DE3) using plasmid pJC20, a kind gift from M. Konrad (Max Planck Institute, Göttingen, Germany), according to the procedure described by Schneider et al. (2000). The protein, stored at −20°C in Tris-HCl, pH 7.5, buffer containing 1 mM DTT, 20 mM KCl, and 50% glycerol was >97% pure as determined by SDS-polyacrylamide gel electrophoresis. The H122G single-mutant and the F64W-H122G double-mutant NDP kinases from *Dictyostelium discoideum* were overexpressed in *E. coli* (XL1-Blue) and purified as described previously for F64W NDP kinase (Schneider et al., 1998). Neither mutant had measurable NDP kinase activity. Protein concentration is expressed as 17 kDa subunits. It was determined either colorimetrically or using (for a 1 mg/ml solution) an absorbance coefficient A_{280} = 0.55 for H122G and A_{280} = 0.85 for F64W-H122G.

Crystallization of the Complex Ribavirin Triphosphate with NDP Kinase and Data Collection. H122G *D. discoideum* NDP kinase in complex with RTP was crystallized by transferring tiny crystals obtained with a higher concentration of PEG, to a drop containing 13% PEG 550 monomethyl ester, 100 mM Tris-HCl, pH 7.5, 30 mM $MgCl_2$, 10 mg/ml protein, and 20 mM RTP, over wells containing 26% PEG 550 monomethyl ester in the same buffer. The crystals belong to the trigonal space group $P3_121$ with unit cell a = b = 71.7 Å, c = 153.8 Å. The asymmetric unit contains a trimer.

X-ray diffraction data from a single crystal were collected at λ = 1.542 Å and 18°C on a Rigaku generator with a MAResearch image plate detector. Diffracted intensities were evaluated with the programs DENZO and SCALEPACK (Otwinowski and Minor, 1997) and further processed using the CCP4 program suite (CCP4, 1994). Overall statistics are given in Table 1. Because the crystals were isomorphous to those of H122G NDP kinase-d4T triphosphate, the 1.85-Å model (Meyer et al., 2000) could be used to calculate phases. Electron density maps were examined using Turbo-FRODO (Roussel and Cambillau, 1991). The first 2Fo-Fc electron density showed clear

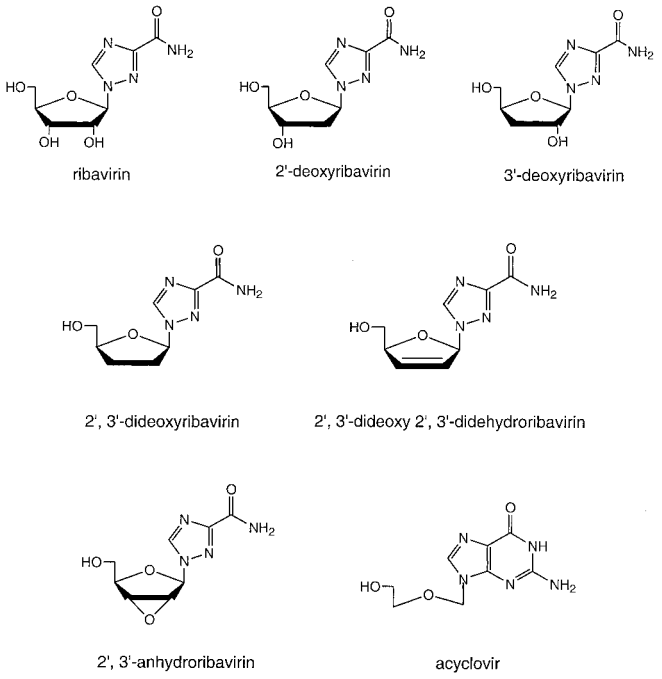

Fig. 1. Chemical structures of ribavirin and derivatives

density for both the protein and the ligand, needing only minor modifications of the protein structure. An RTP molecule and an Mg^{2+} ion are bound to each monomer. Water molecules were gradually added during further conjugate gradient refinement with CNS (Brünger et al., 1998). Residues 2 to 5 are missing in the final model for each monomer.

Fluorometric Binding Studies on NDP Kinase. The affinity of RTP analogs for NDP kinase was determined by following the variation of the intrinsic fluorescence upon nucleotide binding as described previously (Schneider et al., 1998). The fluorescence of the F64W-H122G mutant in T_1 buffer (50 mM Tris-HCl, 75 mM KCl, and 5 mM $MgCl_2$, pH 7.5) was measured at 330 nm with excitation at 310 nm (2-nm excitation slit and 4-nm emission slit) (PTI, New Brunswick, NJ). Successive aliquots of nucleotide were added to a 1 μM enzyme solution. The inner filter effect was negligible. Experimental binding curves were fitted to a quadratic equation after correction for dilution.

Stopped-Flow Kinetic Experiments and Analysis of Kinetic Results. Stopped-flow kinetic experiments were performed with a Hi-Tech DX2 (Salisbury, UK) microvolume stopped-flow reaction analyzer equipped with a high-intensity xenon lamp as described previously (Schneider et al., 1998). The excitation wavelength was 304 nm, with a 2-nm excitation slit and a 320-nm cutoff filter at the emission. Mixing was achieved in less than 2 ms. After mixing NDPK (1 μM) and NTP (10–500 μM), the intrinsic protein fluorescence was recorded for 10–200 s. In each experiment, 400 pairs of data were recorded, and the data from three or four identical experiments were averaged and fitted to a number of nonlinear analytical equations using the software provided by Hi-Tech. All curves fitted to single exponentials.

As described previously (Schneider et al., 1998), the data were analyzed using the reaction scheme:

$$E + NTP \underset{k_{-1}}{\overset{k_{+1}}{\longleftrightarrow}} E \cdot NTP \underset{k_{-2}}{\overset{k_{+2}}{\longleftrightarrow}} E \sim P + NDP$$

The observed single step could be attributed to the phosphotransfer between the nucleotide and the enzyme. Because the product concentration remains very low, the product binding can be neglected. The binding steps are expected to be fast and not detectable in the time range of the stopped-flow experiments. Saturation could not be obtained with the concentrations of nucleotide triphosphate used. Nevertheless, the data are sufficient to determine k_1k_2/k_{-1} or k_2/K_S, where K_S is the dissociation constant of the E·NTP complex. This represents the catalytic efficiency of the enzyme phosphorylation step, equivalent to a second-order rate constant and allowing a reliable comparison of different NDP kinase substrates.

Expression and Purification of HCV 1b Polymerase. The *NS5B* gene encoding HCV 1b polymerase was PCR-amplified using

TABLE 1
Statistics on crystallographic analysis

Parameter	Values
Diffraction data	
Space group	$P3_121$
Asymmetric unit	trimer
Cell parameters a = b, c (Å)	71.7, 153.8
Resolution (Å)	2.9
Measured intensities	93,018
Unique reflections	10,566
I/σ	8.9
Completeness (%)	99.1
R_{sym} (%)[a]	11.7
Refinement	
R_{cryst} (%)[b]	20.7
R_{free} (%)[c]	24.9
Reflections	10,546
Protein atoms	3420
Ligand atoms	90
Solvent atoms	38
Average B (Å^2)	41
Geometry	
Bond length (Å)	0.007
Bond angle (°)	1.4

[a] $R_{sym} = \Sigma|I_i - \langle I\rangle|/\Sigma\ I_i$, where I_i is the intensity of a reflexion, and $\langle I\rangle$ is the average intensity of that reflexion.
[b] $R_{cryst} = \Sigma||F_{obs}| - |F_{calc}||/\Sigma|F_{obs}|$.
[c] 5% of the data was set aside for free *R*-factor calculation.

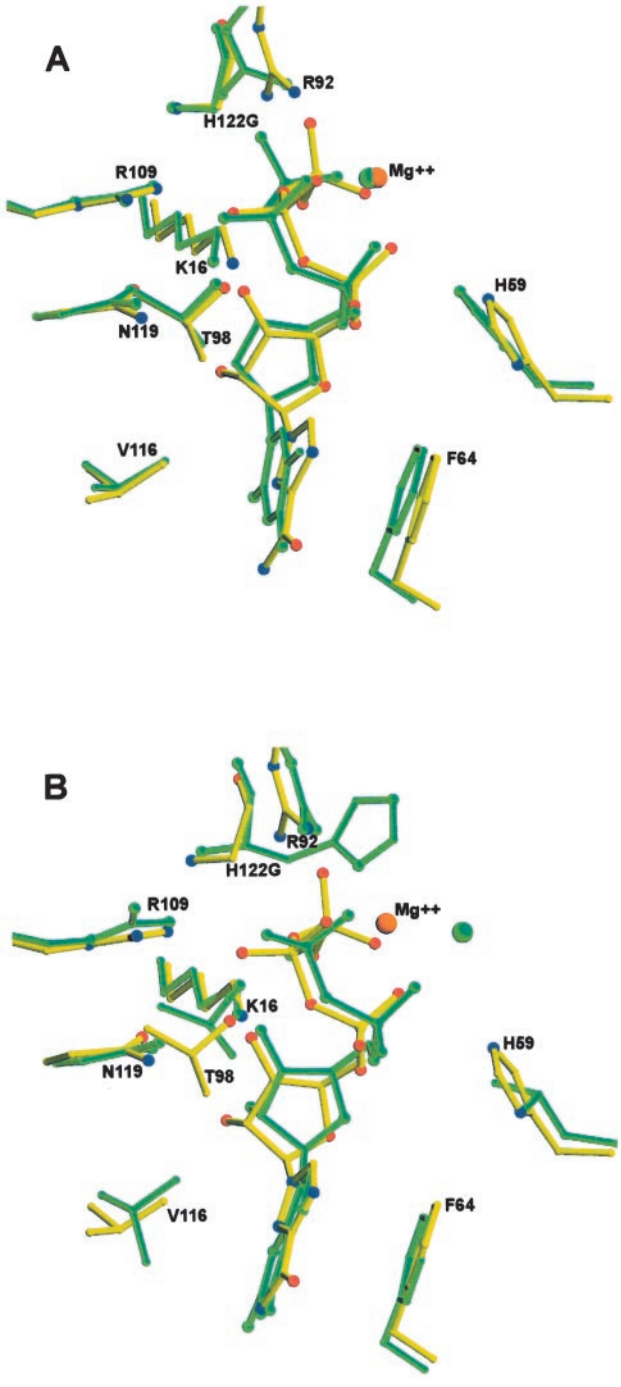

Fig. 2. RTP binding to NDP kinase. RTP bound to the H122G mutant of *D. discoideum* NDP kinase (yellow bonds) is superimposed in (A) to d4T triphosphate (green) bound to the same protein in the 1.85 Å resolution structure determined by (Meyer et al., 2000) in (B), to GDP bound to wild type human NDP kinase B (Morera et al., 1995). The active site histidine is His-122 in *D. discoideum*, His-118 in human. The spheres are Mg^{2+} ions.

the primers HCV-1b-*Bam*HI forward (5′-GGCCGGATCCTCAATGTCCTACACATGGACA-3′) and HCV-1b-*Sal*I reverse (5′-GGCCGTCGACCTAGAGTTTAAGTTTGGATTTTAC-3′) from a clinical HCV isolate serotype 1b to yield Δ55 NS5B 1b cDNA, which specifies an NS5B protein truncated at its C terminus by 55 amino acids. The amplified fragment was digested by *Bam*HI and *Sal*I, cloned into PQE-30 (Amersham Biosciences, Orsay, France), which specifies an N-terminal His_6 tag, and the resulting vector was used to transform BL21pDNAy *E. coli* cells. Bacteria were cultured at 37°C in Luria broth medium supplemented with 100 μg/ml ampicillin and 25 μg/ml kanamycin until $A_{600\ nm}$ reached 0.6. The temperature of the culture was then switched to 27°C, and expression was induced by the addition of 0.3 mM isopropyl β-D-thiogalactoside for 2 h. Bacteria were harvested by centrifugation, washed twice in phosphate-buffered saline, and the pellet was stored at −80°C until use. Bacteria were lysed for 30 min on ice in 3 ml of buffer 1 (50 mM sodium phosphate, pH 7.5, and 20% glycerol) per gram of bacteria supplemented with 1 mg/ml lysozyme, 1 mM phenylmethylsulfonyl fluoride, and 1 mM benzamidine. Lysates were diluted with 3 ml of buffer 2 (50 mM sodium phosphate, pH 7.5, 20% glycerol, 0.6 M NaCl, 10 mM β-mercaptoethanol, 1.6% Igepal, 20 mM imidazole, and 7 μg of DNase) per gram of bacteria, left on ice for 30 min, and sonicated on ice. Lysates were centrifuged for 30 min at 75,000*g*, and the cleared lysates were loaded on a 1-ml Hi-Trap heparin column (Amersham Biosciences). After extensive washes in buffer 3 (50 mM $NaPO_4$, pH 7.5, 10% glycerol, 0.3 M NaCl, 5 mM β-mercaptoethanol, and 10 mM imidazole), bound proteins were eluted with 3 ml of buffer 3 adjusted to 900 mM NaCl. Eluted proteins were then diluted with buffer 3 without NaCl to an NaCl concentration of 0.3 mM and applied to 1.5 ml of a nickel-nitrilotriacetic acid agarose column (QIAGEN, Hilden, Germany). The column was washed extensively before elution of the His_6-tagged HCV polymerase with buffer 3 containing 350 mM imidazole. The fractions containing the HCV polymerase were dialyzed against buffer 3 without imidazole and stored at −20°C.

HIV reverse transcriptase (HIV RT) and phage T7 RNA polymerase (T7 RNAP) were purified as described in by Boretto et al. (2001) and Sousa (2000), respectively.

Polymerase Assays. Polymerase activity was assayed by monitoring the formation of radiolabeled nucleic acid product absorbed onto DE-81 ion exchange paper discs. All radioactive nucleotides come from Amersham Biosciences. For HIV reverse transcriptase experiments, reactions were performed in RT buffer (50 mM Tris-HCl, pH 8.0, 50 mM KCl, 10 mM $MgCl_2$, and 0.05% Triton X-100) at 37°C with a bacteriophage MS2 template (Roche, Meylan, France) annealed to the primer (5′-CTCGGTCAGCTACCGAGGAGA-3′; 20 nM primer/template), dATP, dCTP, and dGTP (10 μM each), decreasing amount of ribavirin or analogs (4 mM, 0.8 mM, 160 μM, 32 μM, 6.4 μM, and 1.3 μM), and 5 μM [^{3}H]dTTP (0.12 μCi of [^{3}H]TTP at 1 μCi/μl). Reactions were initiated by the addition of recombinant RT (50 nM). After 30 min, aliquots were withdrawn and spotted onto DE-81 paper discs. Filter paper discs were washed three times for 10 min in 0.3 M ammonium formate, pH 8.0, washed two times in ethanol, and dried. The radioactivity bound to the filter was determined using liquid scintillation counting.

For phage T7 polymerase experiments, reactions were performed in T7 buffer (40 mM Tris-HCl, pH 7.5, 6 mM $MgCl_2$, 2 mM spermidine, and 10 mM DTT) at 37°C, using 10 ng of DNA template, 1 or 0.5 mM ATP, CTP, UTP, and [α-^{32}P]GTP (0.1 μCi of [^{32}P]GTP at 10 μCi/μl). Reactions were initiated by the addition of 1 μg of recombinant T7 RNAP in presence of 0.5 or 1.5 mM RTP or analogs. Aliquots were withdrawn after 30 min and 1 h and spotted onto DE-81 paper discs. Filter papers were processed as described above.

HCV polymerase experiments were performed in RdRp buffer (50 mM HEPES, pH 8.0, 10 mM KCl, 1 mM $MnCl_2$, 5 mM $MgCl_2$, and 5 mM DTT) containing 125 ng/μl of homopolymeric cytosine RNA template (Amersham Biosciences) annealed to a guanosine dinucleotide primer (ESGS/Cybergene, Evry, France), and 0.5 mM [α-^{32}P]GTP (0.1 μCi of [^{32}P]GTP at 10 μCi/μl). Reactions were initiated by the addition of 300 ng of purified recombinant HCV 1b polymerase and incubated at 30°C. Aliquots were withdrawn overtime and spotted onto DE-81 paper discs. For elongation inhibition, the reaction was incubated without RTP or analogs at 30°C. After 15 min, 0.5 mM RTP or RTP derivatives were added to the samples, and the reaction was allowed to continue for 80 min. Aliquots were withdrawn overtime and spotted onto DE-81 paper discs. The latter were washed and processed as described above. Results shown are representative of three different experiments.

Results

X-Ray Structure of Ribavirin Triphosphate Bound to NDP Kinase. *D. discoideum* NDP kinase has 60 and 58% sequence identity, respectively, with the major A and B isoforms of the human enzyme, also called Nm23-H1 and Nm23-H2 (Lacombe et al., 2000). All eukaryotic NDP kinases are hexamers, including the *D. discoideum* and human pro-

TABLE 2

Polar interactions between RTP and NDP kinase

Distance column shows mean and S.D. of distances (Å) observed in the three subunits present in the asymmetric unit of the H122G-RTP crystals. ADP-BeF_3 column shows distances observed in the 2.3-Å crystal structure of the wild-type *D. discoideum* NDP kinase in complex with ADP and beryllium fluoride (Xu et al., 1997).

RTP	Protein	Distance	ADP-BeF_3
		Å	
Ribose			
O2′	NZ Lys 16	3.5 (0.2)	3.2
O3′	NZ Lys 16	2.8 (0.1)	2.9
	ND2 Asn 119	3.0 (0.1)	2.9
	O3B[a]	3.2 (0.4)	2.6
α-Phosphate O2A	NE His 59	3.2 (0.1)	3.0
	Mg^{2+}	2.1 (0.2)	2.2
β-Phosphate	NH2 Arg 92	3.0 (0.2)	3.1
O1B	Mg^{2+}	2.4 (0.4)	2.3
O2B	NH1 Arg 109	3.1 (0.1)	3.1
	NH1 Arg 109	3.3 (0.3)	3.1
γ-Phosphate[b]	NZ Lys 16	2.9 (0.1)	2.9
O1G	OH Tyr 56	2.9 (0.3)	2.5
O2G	N Gly 123	2.8 (0.1)	3.1
O3G	Mg^{2+}	2.3 (0.4)	2.2

[a] Oxygen bridging the β- and γ-phosphates in RTP and O7 in ADP-BeF_3.
[b] Fluoride ions in ADP-BeF_3.

teins. Their subunit folds are very similar, and their active sites are essentially identical (Janin et al., 2000). Structural data show the same mode of binding for GDP to human NDP kinase B (Morera et al., 1995) and ADP or TDP to wild-type *D. discoideum* NDP kinase (Cherfils et al., 1994; Morera et al., 1994). Thus, the *D. discoideum* enzyme is a good model of human NDP kinase for functional studies. In addition, the H122G mutant is useful when studying nucleoside triphosphate binding, because the substitution of the active site histidine prevents transfer of the γ-phosphate to the protein. We previously used the mutant in the analysis of a complex with d4T triphosphate at 1.85-Å resolution (Meyer et al., 2000). With the wild-type protein, bound ATP can be mimicked by a complex of ADP and either aluminum or beryllium fluoride (Xu et al., 1997). The present X-ray structure of H122G in complex with ribavirin triphosphate has an *R* factor of 20.7% (R_{free} = 24.9%) at 2.9 Å resolution and good stereochemistry (Table 1). The protein has essentially the same conformation as in the d4T triphosphate complex, a superposition yielding a RMS distance of 0.26 Å for all equivalent Cα positions. The superposition with GDP-bound human NDP kinase B is almost as good, with an RMS distance of 0.41 Å, excluding nine C-terminal residues that differ in conformation between the *D. discoideum* and human proteins (Lacombe et al., 2000).

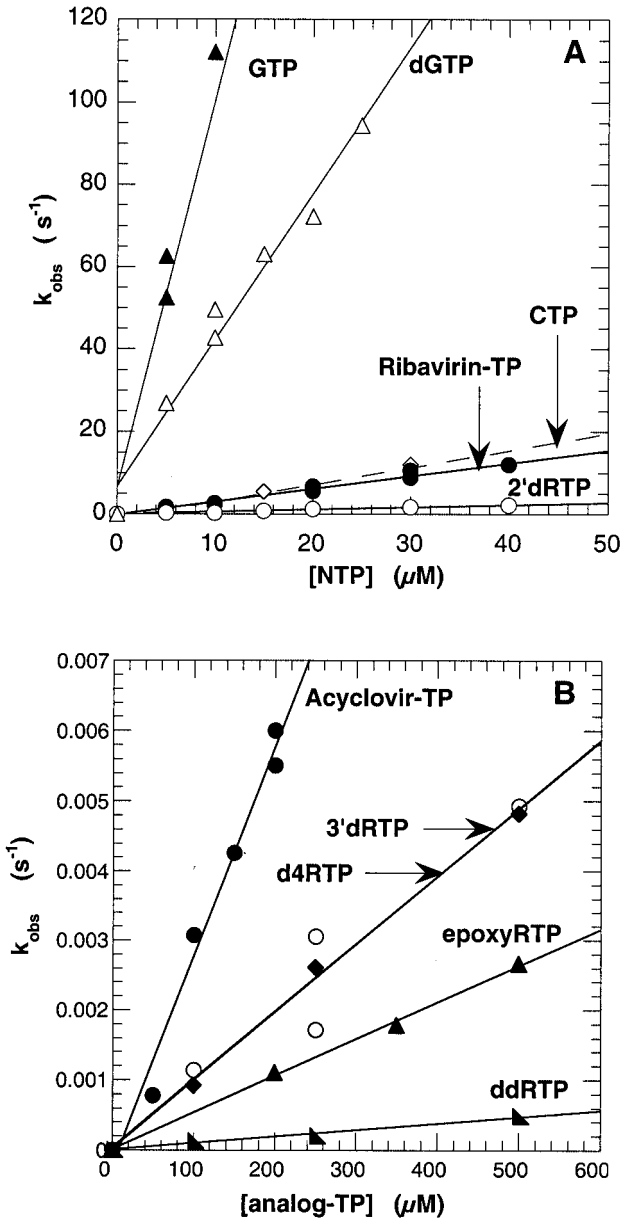

Fig. 3. Pre–steady-state kinetics of NDP kinase phosphorylation by ribavirin triphosphate and analogs. Concentration dependence of the first-order rate constant of NDP kinase phosphorylation by ribavirin triphosphate and analogs. NDP kinase A (1 μM) was rapidly mixed at 20°C with 5 to 50 μM ribavirin or natural substrates (A) or with 5 to 500 μM ribavirin triphosphate analogs (B), and the rates of phosphorylation were measured with a fluorescence stopped-flow device.

RTP binds in the same site and orientation as other nucleotide substrates or nucleotide analogs (Fig. 2). The substituted triazole that replaces the base is in a slit opening on the protein surface and stacks between the side chains of Val-116 and Phe-64. The 2.9-Å electron density map uniquely defines the plane of the five-membered ring, but it is compatible with a 180° rotation of the ring about the glycosidic bond. Thus, the complex may contain either the *syn* and *anti* conformers of the nucleoside analog or a mixture of the two. In addition, the carboxamide group in C3 of the triazole can also flip by 180° relative to the ring. None of these rotations enables the substituted triazole to make polar interactions with the protein. In the GDP complex, guanine makes a hydrogen bond with the side chain carboxylate of the C-terminal glutamate of an adjacent subunit in the hexamer. The distance of the carboxylate to the carboxamide group in C3 of the triazole is more than 5 Å, too long for a hydrogen bond.

Unlike d4T, which has a double bond and no hydroxyl in C2′-C3′, ribavirin carries an unmodified ribose. The sugar in bound RTP has the same 3′-endo ring pucker as in ADP bound to *D. discoideum* NDP kinase (Morera et al., 1994) or GDP in the human enzyme (Morera et al., 1995). The 2′- and 3′-hydroxyl groups make the same interactions as in these two complexes (i.e., with the amide group of Asn-119 and the amino group of Lys-16). All polar interactions that involve the phosphate groups are also conserved (Table 2). The γ-phosphate of RTP, like that of d4T triphosphate (Meyer et al., 2000) interacts with Lys-16, Tyr-56, and the main chain NH of Gly-123. In the wild-type protein, fluoride ions make the same interactions in the ADP-beryllium and aluminum fluoride complexes (Xu et al., 1997).

All the complexes cited above contain a Mg^{2+} ion. The metal interacts with oxygens of two phosphates if the ligand is a diphosphate and oxygens of three phosphates if it is a triphosphate, which is the case of RTP. In either case, water molecules complete the octahedral coordination. The metal takes two positions approximately 2 Å apart in the complexes with di- and triphosphates, illustrated in Fig. 2, respectively, by the human NDP kinase B-GDP and the H122G-RTP structures. The metal-oxygen distances remain in the range 2.0 to 2.4 Å and the phosphate groups themselves do not move: the α- and β-phosphates of bound RTP and GDP superimpose to within 0.5 Å (that is, within the error in the coordinates of a X-ray structure at 2.9 Å resolution).

Catalytic Efficiencies of NDP Kinase for Ribavirin Triphosphate and Derivatives. We followed the time course of the reaction of RTP with human NDP kinase A in fast kinetic experiments by monitoring the intrinsic fluorescence of the protein. The fluorescence is quenched upon phosphorylation of the active site histidine by a NTP substrate

TABLE 3

NDP kinase binding and activation of nucleotide analogs

The phosphotransfer reaction between human NDP kinase A and nucleotide analogs was studied in the direction NTP + E → E-P + NDP. Note that ribavirin is in the same range of activity as natural nucleotides, whereas 3′-deoxy derivatives lose most of their efficiency. The F64W-H122G variant of *D. discoideum* is designed to measure NTP binding in the absence of phosphotransfer. Protein fluorescence (λ_{exc} = 310 nm, λ_{em} = 330 nm) increases by 50% upon binding saturation amounts of NTP at 20°C in 50 mM Tris-HCl, 5 mM $MgCl_2$, 75 mM KCl, 1 mM DTT, and 5% glycerol, pH 7.5. K_D values are estimated by fitting the binding curve to a quadratic equation.

Nucleotide	Catalytic Efficiency	K_D
	$M^{-1}\,s^{-1}$	μM
GTP	$(8.0 \pm 1.0) \times 10^6$ (3)	0.15 ± 0.05 (3)
2′ dGTP	$(4.7 \pm 1.0) \times 10^6$ (3)	
CTP	$(4.2 \pm 0.3) \times 10^5$ (3)	7 ± 1 (3)
RTP	$(3.1 \pm 0.2) \times 10^5$ (3)	24 ± 5 (3)
2′ dRTP	$(5.7 \pm 0.2) \times 10^4$ (2)	40 ± 5 (3)
Acyclovir-TP	30.0 ± 2.0 (2)	
3′ dRTP	10.0 ± 0.5 (2)	250 ± 10 (3)
d4RTP	10.0 ± 0.8 (2)	200 ± 20 (3)
EpoxyRTP	5.0 ± 1.0 (2)	980 ± 50 (3)
ddRTP	1.0 ± 0.2 (2)	2500 ± 1000 (3)

and, reciprocally, enhanced upon its dephosphorylation by NDP (Deville-Bonne et al., 1996). The reaction with RTP yields a monoexponential fluorescence decay without a lag, as previously reported for other nucleoside triphosphates (Schaertl et al., 1998; Schneider et al., 1998). The pseudo–first-order constant k_{obs} of the exponential decay increased linearly with RTP concentrations in the range investigated (5–50 μM) (Fig. 3). The slope of the linear fit, which measures the catalytic efficiency of RTP as a substrate for NDP kinase, was $k_2/K_S = 3 \times 10^5\ M^{-1}s^{-1}$. This makes RTP a good substrate, comparable with the natural substrate CTP, although inferior to GTP, which is the best known substrate of NDP kinase (Table 3).

The phosphorylation kinetics were also studied with RTP analogs modified on the ribose. The absence of a 2′-hydroxyl group in 2′dRTP led to a 5-fold loss in catalytic efficiency, comparable with the 2-fold change observed between GTP and dGTP (Fig. 3A and Table 2). Removal of the 3′-hydroxyl group had a much larger effect, causing a drop in activity by a factor of 10^4 with both 3′dRTP and d4RTP. The factor reached 10^5 in the case of the 2′,3′-dideoxy analog (ddRTP) (Fig. 3B and Table 2). Very similar observations have been made with thymidine analogs: the d4T derivative was 10-fold better that the dideoxy derivative when tested as a substrate of NDP kinase (Schneider et al., 2000). The 2′3′-epoxy analog of RTP (epoxyRTP) is also better than the dideoxy compound. Acyclovir triphosphate was also assayed for reaction with NDP kinase. Acyclovir, which is used in herpes virus therapy, is a guanosine analog with a linear connection between the base and 5′-hydroxyl group. The phosphorylation reaction followed in the fluorescence test was 10^5 times slower than for GTP and 10^4 times slower than for RTP. This confirms the dominant role of the sugar hydroxyl groups and the minor importance of the base in the reaction with NDP kinase.

Binding Affinities of Ribavirin Triphosphate and Derivatives for NDP Kinase. Although the equilibrium dissociation constant K_S of the NDP kinase-NTP complex is not accessible in these kinetic experiments, it can be estimated by using a mutant NDP kinase, which lacks the cat-

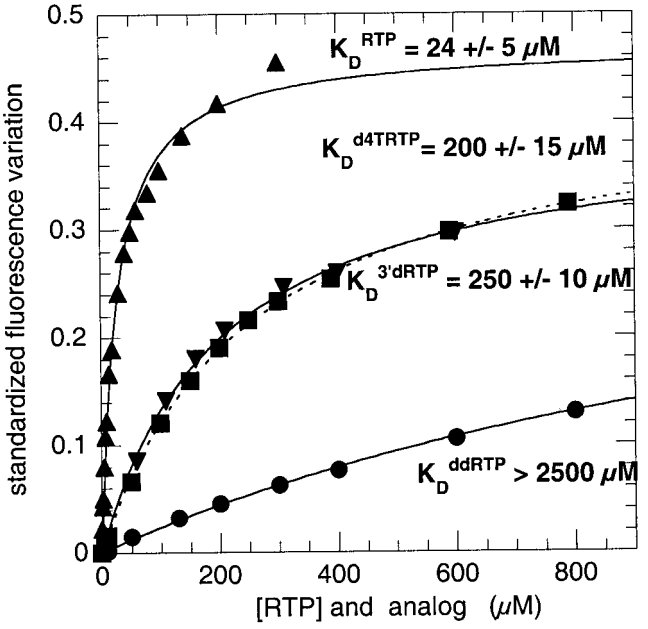

Fig. 4. Binding affinity of ribavirin triphosphate and analogs for NDP kinase. Fluorescence titration curve of F64W-H122G mutant NDP kinase (1 μM) by RTP or analogs at 20°C. Solid lines represent the best fit of the data to a quadratic saturation curve. The apparent K_D values are shown.

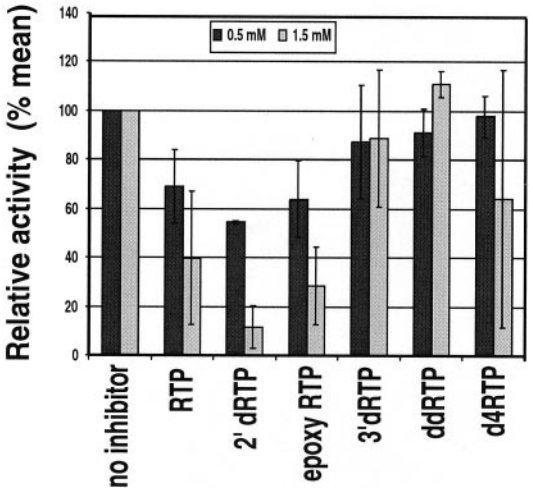

Fig. 5. Inhibition of HCV NS5B polymerase by RTP and its ribose-modified derivatives. Assays were performed in the presence of 125 ng/μl of template/primer [poly(C)/GG] and 0.5 or 1.5 mM RTP or analogs. Relative activities were determined by calculating the slope of the incorporation linear phase occurring after the lag phase (see *Inhibition of Viral Polymerase by RTP and Analogs*). Mean values of relative activities for each compound are shown as percentage of NS5B activity without inhibitor. S.E. and mean values were calculated from two independent experiments.

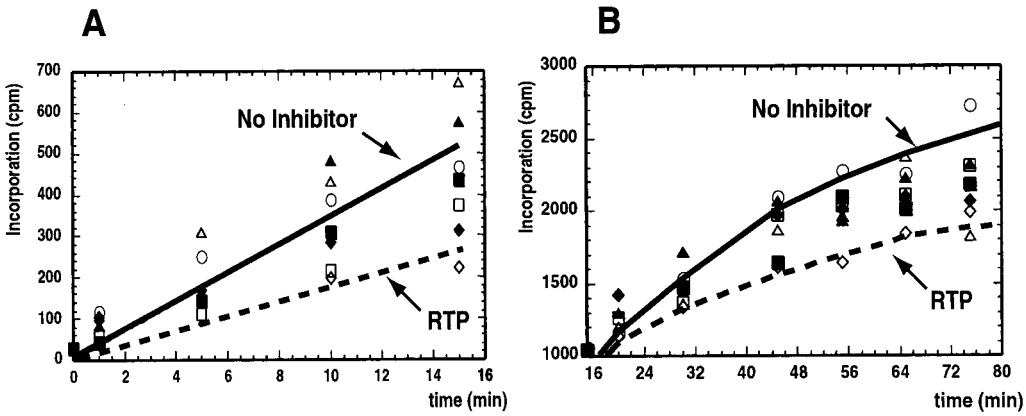

Fig. 6. Inhibition of initiation or elongation of HCV polymerase by RTP and derivatives. Assays were performed in the presence of 125 ng/μl of template/primer [poly(C)/GG] and 0.5 mM of RTP or analogs (○, no inhibitor; ◇, RTP; ◆, 2′dRTP; ■ 3′dRTP; □, epoxyRTP; ▲, ddRTP; △, d4RTP). For inhibition of initiation, polymerase activity was determined as incorporation of radiolabeled GTP nucleotide during the first 15 min. For inhibition of elongation, polymerase reaction was started without RTP derivatives. After 15 min, 0.5 mM RTP or derivatives were added, and the reaction continued for 80 min. Polymerase activity was determined as incorporation of radiolabeled GTP nucleotide over time.

alytic histidine and where the phenylalanine (Phe-64 in *D. discoideum NDP* kinase) stacking on the base is replaced by a tryptophan. In the H122G-F64W double mutant, the protein fluorescence changes upon nucleotide binding although no phosphorylation takes place. Titration by RTP yielded $K_S = 24 \pm 5$ μM, a 3-fold decrease in affinity relative to CTP and 160-fold relative to GTP (Table 3). RTP analogs with a modified sugar showed a further decrease in affinity by a factor of 2 for 2′dRTP, 10 for 3′dRTP and d4RTP, and 100 for ddRTP. Although smaller than for the catalytic efficiency k_2/K_S, these ratios indicate that all analogs bind NDP kinase with lower affinities than the natural substrates.

Inhibition of Viral Polymerase by RTP and Analogs. Ribavirin has been reported to exhibit some anti-HIV activity, but its combination with other nucleotide analogs leads to serious adverse effects (Sim et al., 1998). Indeed, although ribavirin is a ribonucleoside analog, RTP may also inhibit the DNA polymerase activity of HIV RT. Because 2′,3′-dideoxynucleotides are efficient against HIV RT, it was of interest to test whether 2′- or 3′-deoxy-modified RTP is efficient against HIV RT and retains inhibitory power against HCV polymerase.

We first analyzed the activity of RTP and derivatives against DNA polymerization by HIV RT. Because RMP can be incorporated opposite either cytidine or uridine, we used templates containing all four natural ribonucleotides. HIV RT was not affected by any of the compounds at concentration up to 4 mM (data not shown), suggesting that they are either not incorporated or not chain terminators. We next tested whether ribavirin derivatives inhibit RNA polymerases. Phage T7 RNAP is the best known RNA polymerase and constitutes an interesting model for inhibition. Polymerization was assayed using a DNA template containing the T7 promotor, the four natural nucleotides, and increasing amounts of RTP or derivatives. No significant polymerization inhibition was observed, suggesting that RTP and derivatives are not inhibitors of T7 RNA polymerase (data not shown).

RTP and derivatives were then tested against HCV polymerase. HCV polymerase activity is characterized by a nonprocessive initiation step, followed after 10 to 15 min by linear incorporation (elongation step). We measured the nucleotide incorporation over time in presence of RTP or RTP analogs. Polymerase activity was determined by calculating the rate of nucleotide incorporation after the initiation step. RTP, 2′dRTP, and epoxyRTP inhibited HCV polymerase; 2′dRTP was the most efficient (Fig. 5, 85% of relative inhibition). The other RTP analogs inhibited HCV polymerase weakly, if at all.

We wanted next to test whether the lower nucleotide incorporation was caused by the initiation or elongation step. During the first 15 min, we observed a decrease of nucleotide

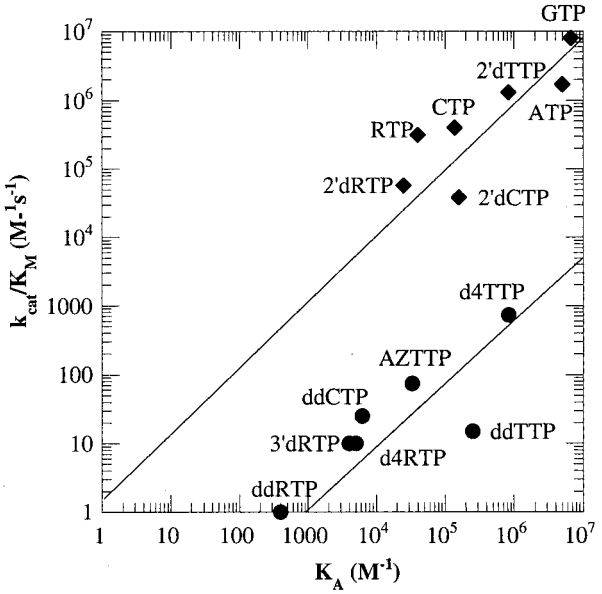

Fig. 7. Correlation of catalytic efficiencies of NDP kinase for several nucleotides triphosphate and their binding affinities. The equilibrium affinity constant K_A is measured from fluorescence titrations curves on F64W-H122G mutant NDP kinase as shown on Fig. 4. Catalytic efficiencies are obtained in stopped-flow experiments with human NDP kinase A. The active site of both enzymes is highly conserved (Janin et al., 2000). AZTTP, 3′-azidothymidine triphosphate; d4TTP, 2′,3′-dideoxy-2′,3′-didehydrothymidine triphosphate; ddCTP, 2′,3′-dideoxycytidine triphosphate; 2′dTTP, 2′-deoxythymidine triphosphate; 2′dRTP, 2′-deoxyribavirin triphosphate; 2′dCTP, 2′-deoxycytidine triphosphate; 3′dRTP, 3′-deoxyribavirin triphosphate; ddTTP, 2′,3′-dideoxythymidine triphosphate; d4RTP, 2′,3′-dideoxy-2′,3′-didehydroribavirin triphosphate; ddRTP, 2′,3′-dideoxyribavirin triphosphate.

incorporation induced by RTP, epoxyRTP, and 2′dRTP, whereas 3′dRTP, ddRTP, or d4RTP had no effect or a slight activating effect (Fig. 6A). To measure inhibition of the elongation step, RTP analogs were added after 15 min at the end of the initiation step, and the reaction continued for 80 min. Under these conditions, elongation was inhibited only by RTP, with little effect of the other analogs (Fig. 6B).

In summary, RTP inhibits both initiation and elongation, 2′dRTP and epoxy-RTP act only on initiation, and 3′dRTP, ddRTP, and d4RTP have no effect on nucleotide incorporation. This suggests that both the 3′ and 2′ hydroxyl groups are required for inhibiting elongation but that the presence of an oxygen at the 3′ position is sufficient for inhibiting initiation.

Discussion

Unlike nucleoside analogs directed against HIV RT, which lack a 3′OH, ribavirin contains a normal ribose moiety and cannot act as a chain terminator. The derivatives tested here combine the base modification of ribavirin and some of the sugar modifications found in RT inhibitors. We tested the capacity of NDP kinase to produce the triphosphate form of these derivatives and the effect of the triphosphate form on several target viral polymerases.

Correlation between Binding Affinities and Catalytic Efficiencies of Nucleotides for NDP Kinase. RTP and its analogs were found to be excellent substrates for NDP kinase on the condition that the 3′hydroxyl group is present. This is in line with previous studies of natural substrates and analogs. Figure 7 shows a correlation between the catalytic efficiencies and the equilibrium association constant K_A for natural nucleotides and analogs. Substrates are found to belong to two classes: those carrying a 3′-OH and those lacking this hydroxyl group. The two lines obtained for the two classes indicate a change in catalytic efficiency by a factor 500 to 1000, illustrating the well-established contribution of the 3′-OH to substrate-assisted catalysis by NDP kinase. The lines themselves show that, within each class, the catalytic efficiency correlates linearly to the binding affinity.

Tighter substrate binding makes for more efficient phosphotransfer. Thus, GTP has both the highest reactivity and the best affinity (K_D = 0.15 μM). Affinity and reactivity are less for RTP. The structures of GDP bound to the active enzyme and RTP bound to the H122G variant (Fig. 1) suggest a simple reason for the difference: the ribavirin base, which is smaller than guanine or other natural bases, buries less surface upon binding the enzyme. Thus, the nonpolar contribution to the binding energy is less, whereas other interactions are conserved. All complexes of NDP kinase with nucleotides (at least 10 X-ray structures are known) indicate a similar mode of binding for all, except for the presence or absence of the 2′-OH, and the size of the base surface in nonpolar contact with the protein. Both the polar interactions made by the 3′OH and the nonpolar contact contribute to hold the substrate in place.

The Use of Ribavirin Nucleotide as RNA Polymerization Inhibitors. Ribavirin is currently used as a therapeutical agent against HCV in combination with interferon (Lauer and Walker, 2001). Although it is a weak antiviral drug when used alone, ribavirin is phosphorylated by cellular kinases up to the triphosphate level, and ribavirin monophosphate is incorporated into the viral RNA by the recombinant HCV polymerase (Maag et al., 2001). Templates containing RMP can also block RNA elongation. This makes ribavirin an interesting candidate for chemical modification aiming to increase its antiviral effect.

The RNA replication of the HCV genome goes through two steps relevant to our discussion: the initiation step, comprising the incorporation of the very first nucleotide, up to the 4th or 5th nucleotides, and the elongation step, which consists of processive extension of the neosynthesized RNA. The initiation step, and especially the synthesis of the first phosphodiester bond between the two first nucleotides, is nonprocessive and rate-limiting (Kao et al., 2001). Moreover, the switch from initiation to elongation requires a conformational change. Therefore, polymerization can be inhibited during the initiation step, by preventing the switch from initiation to elongation, or during processive synthesis. We have observed that 2′dRTP and epoxyRTP are HCV polymerase inhibitors if they are present at the beginning of the reaction, but not if they are added after 15 min of reaction. This suggests that 2′dRTP and epoxyRTP are initiation inhibitors only. 3′dRTP, ddRTP, and d4RTP, which were thought to be chain terminators, do not have the expected inhibitory effect, during either initiation or elongation, suggesting that they are not incorporated by the HCV enzyme. In contrast, RTP inhibits both initiation and elongation.

What is the detailed mechanism of this inhibitory effect? HCV polymerase activity is stimulated in the presence of high concentrations of GTP (Lohmann et al., 1998), and kinetic studies revealed two K_M values for GTP, one similar to that of other nucleotides, and a higher one (Luo et al., 2000). Because ribavirin is a guanosine analog, it can compete either for the incorporation of GTP in the nascent RNA or for the stimulating effect of GTP. Recently, an allosteric GTP-binding site has been characterized far away from the catalytic site and is not involved in the polymerization reaction (Bressanelli et al., 2002). This allosteric GTP-binding site might also represent a target for GTP analogs. Indeed, because RTP, epoxyRTP, and 2′dRTP inhibit the initiation step of the polymerization, they may compete for this GTP-binding site and may inhibit the allosteric activation or the switch from initiation to elongation, normally induced by the binding of GTP to this site.

Epoxy-RTP, which does not carry a 3′-OH, is a putative chain terminator, but it does not show the expected effect, at least during the elongation step of polymerization. RTP and 2′dRTP carry a 3′-OH and should not be chain terminators. Nevertheless, they, like epoxy-RTP, inhibit the initiation of synthesis by HCV polymerase. This suggests that a 3′-hydroxyl group, or at least the presence of an oxygen at the 3′ position, is required to inhibit this step. Inhibition of elongation requires both hydroxyls in position 2′ and 3′, making RTP the only efficient inhibitor of this step. RTP may act at either step by competing for the NTP binding site or by blocking incorporation per se, as already observed by Maag et al. (2001).

In conclusion, the experiments suggest that 2′-deoxy ribavirin may be an alternative to ribavirin in therapies against C hepatitis. It is efficiently activated to the triphosphate form by NDP kinase and is a potent specific inhibitor of HCV polymerase initiation. The absence of the 2′OH on 2′deoxyribavirin is likely to result in a weaker interaction with

IMP dehydrogenase, the cytotoxic cellular target, because the active site side chains interact with both 2′OH and 3′OH of the nucleotide (Colby et al., 1999). Cellular studies are now needed to validate this in vitro study.

Acknowledgments

We gratefully acknowledge C. Meier (Universität Hamburg, Hamburg, Germany) for kindly providing ribavirin. We thank S. Sarfati (Unité de Chimie Organique, Institut Pasteur) for initial input in the work and Céline Boulard for excellent technical assistance. We are deeply indebted to Sonia Longhi for mutagenesis experiments to reduce the number of rare codons in the HCV polymerase cDNA.

References

Boretto J, Longhi S, Navarro JM, Selmi B, Sire J, and Canard B (2001) An integrated system to study multi-substituted human immunodeficiency virus type I reverse transcriptase. *Anal Biochem* **292:**139–147.

Bourdais J, Biondi R, Lascu I, Sarfati S, Guerreiro C, Janin J, and Veron M (1996) Cellular phosphorylation of anti-HIV nucleosides: role of nucleoside diphosphate kinase. *J Biol Chem* **271:**7887–7890.

Bressanelli S, Tomei L, Rey FA, and De Francesco R (2002) Structural analysis of the hepatitis C virus RNA polymerase in complex with ribonucleotides. *J Virol* **76:** 3482–3492.

Brünger AT, Adams PD, Clore GM, DeLano WL, Gros P, Grosse-Kunstleve RW, Jiang JS, Kuszewski J, Nilges M, Pannu NS, et al. (1998) Crystallography & NMR system: A new software suite for macromolecular structure determination. *Acta Crystallogr Sect D Biol Crystallogr* **54:**905–921.

CCP4 (1994) Collaborative project No. 4. *Acta Crystallogr Sect D Biol Crystallogr* **50:**760–763.

Cherfils J, Morera S, Lascu I, Veron M, and Janin J (1994) X-ray structure of nucleoside diphosphate kinase complexed with dTDP and Mg^{2+} at 2-Å resolution. *Biochemistry* **33:**9062–9069.

Colby TD, Vanderveen K, Strickler MD, Markham GD, and Goldstein BM (1999) Crystal structure of human type II inosine monophosphate dehydrogenase: implications for ligand binding and drug design. *Proc Natl Acad Sci USA* **96:**3531–3536.

Crotty S, Maag D, Arnold JJ, Wong W, Lau JYN, Hong Z, Andino R, and Cameron CE (2000) The broad-spectrum antiviral ribonucleoside ribavirin is an RNA virus mutagen. *Nature (Lond) Med* **6:**1375–1379.

Deville-Bonne D, Sellam O, Merola F, Lascu I, Desmadril M, and Veron M (1996) Phosphorylation of nucleoside diphosphate kinase at the active site studied by steady-state and time-resolved fluorescence. *Biochemistry* **35:**14643–14650.

Homma M, Jayewardene AL, Gambertoglio J, and Aweeka F (1999) High-performance liquid chromatographic determination of ribavirin in whole blood to assess disposition in Erythrocytes. *Antimicrob Agents Chemother* **43:**2716–2719.

Janin J, Dumas C, Moréra S, Xu Y, Meyer P, Chiadmi M, and Cherfils J (2000) Three-dimensional structure of nucleoside diphosphate kinase. *J Bioenerg Biomemb* **32:**215–225.

Jarvis SM, Thorn JA, and Glue P (1998) Ribavirin uptake by human erythrocytes and involvement of nitrobenzylthioinosine-sensitive (es)-nucleoside transporters. *Br J Pharmacol* **123:**187–1502.

Kao CC, Singh P, and Eckert DJ (2001) De novo initiation of viral RNA-dependent RNA synthesis. *Virology* **287:**251–260.

Lacombe ML, Milon L, Munier A, Mehus JG, and Lambeth DO (2000) The human Nm23/nucleoside diphosphate kinases. *J Bioenerg Biomemb* **32:**247–258.

Lauer GM and Walker BD (2001) Hepatitis C virus infection. *N Engl J Med* **345:** 41–52.

Lohmann V, Roos A, Körner F, Koch JO, and Bartenschlager R (1998) Biochemical and kinetic analyses of NS5B RNA-dependent RNA polymerase of the hepatitis C virus. *Virology* **249:**108–118.

Ludwig J and Eckstein F (1989) Rapid and efficient synthesis of nucleoside 5′-*O*-(1-thiotriphosphates), 5′-triphosphates and 2′,3′-cyclophosphorothioates using 2-chloro-4H-1,3,2-benzodioxaphosphorin-1-one. *J Org Chem* **54:**631–635.

Luo G, Hamatake RK, Mathis DM, Racela J, Rigat KL, Lemm J, and Colonno RJ (2000) De novo initiation of RNA synthesis by the RNA-dependent RNA polymerase (NS5B) of hepatitis C virus. *J Virol* **74:**851–863.

Maag D, Castro C, Hong Z, and Cameron CE (2001) Hepatitis C virus RNA-dependent RNA polymerase (NS5B) as a mediator of the antiviral activity of ribavirin. *J Biol Chem* **276:**46094–46098.

McHutchison J, Gordon S, and Schiff E (1998) Interferon alfa-2b alone or in combination with ribavirin as initial treatment for chronic hepatitis C. Hepatitis Interventional Therapy Group. *N Engl J Med* **1998:**1485–1492.

Meier C and Huynh-Dinh T (1991) Improved conversion of adenosine to 3′-deoxyadenosine. *Synlett* **4:**227–228.

Meyer P, Schneider B, Sarfati S, Deville-Bonne D, Guerreiro C, Boretto J, Janin J, Veron M, and Canard C (2000) Structural basis for activation of α-boranophosphate nucleotide analogues targeting drug-resistant reverse transcriptase. *EMBO J* **19:**3520–3529.

Morera S, Lacombe M-L, Xu Y, LeBras G, and Janin J (1995) X-Ray structure of nm23 human nucleoside diphophate kinase B complexed with GDP at 2Å resolution. *Structure* **3:**1307–1314.

Morera S, Lascu I, Dumas C, LeBras G, Briozzo P, Veron M, and Janin J (1994) ADP binding and the active site of nucleoside diphosphate kinase. *Biochemistry* **33:** 459–467.

Otwinowski Z and Minor W (1997) Processing of X-ray diffraction data collected in oscillation mode. *Methods Enzymol* **276:**307–326.

Page T and Conner JD (1990) The metabolism of ribavirin in erythrocytes and nucleated cells. *Int J Biochem* **22:**379–383.

Parks RE Jr and Agarwal RP (1973) Nucleoside diphosphokinases, in *The Enzymes* (Boyer PD ed) Vol. 8, pp 307–334, Academic Press, New York.

Patil SD, Ngo LY, Glue P, and Unadkat JD (1998) Intestinal absorption of ribavirin is preferentially mediated by the Na^+-nucleoside purine (N1) transporter. *Pharm Res* **15:**950–952.

Patterson JL and Fernandez-Larsson R (1990) Molecular mechanisms of action of ribavirin. *Rev Infect Dis* **12:**1139–1146.

Pochet S and Dugué L (1998) Imidazole-4-carboxamide and 1, 2, 4-triazole-3-carboxamide deoxynucleotides as simplified building DNA building blocks with ambiguous pairing capacity. *Nucleosides and Nucleotides* **17:**2003–2009.

Poynard T, Marcellin P, and Lee S (1998) Randomised trial of interferon a-2b plus ribavirin for 48 weeks or for 24 weeks versus interferon a-2b plus placebo for 48 weeks for treatment of chronic infection with hepatitis C. *Lancet*: 1426–1432.

Roussel A and Cambillau C (1991) *Silicon Graphics Directory.* Silicon Graphics, Mountain View, CA.

Schaertl S, Konrad M, and Geeves MA (1998) Substrate specificity of human nucleoside-diphosphate kinase revealed by transient kinetic analysis. *J Biol Chem* **273:**5662–5669.

Schneider B, Biondi R, Sarfati R, Agou F, Guerreiro C, Deville-Bonne D, and Veron M (2000) The mechanism of phosphorylation of anti-HIV D4T by nucleoside diphosphate kinase. *Mol Pharmacol* **57:**948–953.

Schneider B, Xu YW, Sellam O, Sarfati R, Janin J, Veron M, and Deville-Bonne D (1998) Pre-steady state of reaction of nucleoside diphosphate kinase with anti-HIV nucleotides. *J Biol Chem* **273:**11491–11497.

Sim SM, Hoggard PG, Sales SD, Phiboonbanakit D, Hart CA, and Back DJ (1998) Effect of ribavirin on zidovudine efficacy and toxicity *in vitro*: a concentration-dependent interaction. *AIDS Research and Human retroviruses* **14:**1661–1667.

Sintchak MD and Nimmesgern E (2000) The structure of inosine 5′-monophosphate dehydrogenase and the design of novel inhibitors. *Immunopharmacology* **47:**163–184.

Sousa R (2000) Use of T7 RNA polymerase and its mutants for incorporation of nucleoside analogs into RNA. *Methods Enzymol* **317:**6–74.

Upadhya K, DaRe J, Schubert EM, Chmurny GN, and Gabrielsen B (1990) Preparation and antiviral activity of several deoxygenated ribavirin and thiazofurin derivatives. *Nucleos Nucleot* **9:**649–662.

Witkowski JT, Robins RK, Sidewell R, and Simon L (1972) Design, synthesis and broad spectrum antiviral activity of 1-β-D-ribofuranosyl-1,2,4-triazole-3-carboxamide and related nucleosides. *J Med Chem* **15:**1150–1154.

Wray SK, Gilbert BE, and Knight V (1985) Effect of ribavirin triphosphate on primer generation and elongation during influenza virus transcription *in vitro. Antivir Res* **5:**39–48.

Xu Y, Morera S, Janin J, and Cherfils J (1997) AlF_3 mimics the transition state of protein phosphorylation in the crystal structure of nucleoside diphosphate kinase and MgADP. *Proc Natl Acad Sci USA* **94:**3579–3583.

Address correspondence to: Dominique Deville-Bonne, Régulation Enzymatique des Activités Cellulaires, Departement Biologie Structurale et Chimie, Institut Pasteur, 25 rue du Dr. Roux 75724, Paris Cedex 15 France. E-mail: ddeville@pasteur.fr